Desalination and Water Treatment
www.deswater.com

doi: 10.5004/dwt.2023.29862

307 (2023) 130–139
September

Adsorption separation *in-situ* synthesis of MIL-101(Cr)/AC composite and its cycling adsorption for Cr(VI) from aqueous solution

Zhuannian Liu*, Yue Li, Yingying Teng

College of Geology and Environment, Xi'an University of Science and Technology, Xi'an 710054, PR China, emails: liuzhuannian@163.com (Z. Liu), 1165748150@qq.com (Y. Li), 851950658@qq.com (Y. Teng)

Received 19 January 2023; Accepted 23 July 2023

ABSTRACT

Cr(III) was adsorbed and separated by activated carbon (AC) from aqueous solution in order to recycle and reuse it, then MIL-101(Cr)/AC composite was *in-situ* synthesized by hydrothermal method based on AC adsorbed Cr(III). The structure and morphology of AC, MIL-101(Cr) and MIL-101(Cr)/AC composite were investigated by X-ray diffraction, Fourier-transform infrared spectroscopy, scanning electron microscopy, Brunauer–Emmett–Teller and zeta potential. The factors of time, temperature, pH and adsorbent dosage on Cr(VI) adsorption capacity and the reusability of the materials were studied. The results indicated that the specific surface area of AC, MIL-101(Cr) and MIL-101(Cr)/AC was 950.9, 1,687.1 and 655.9 $m^2 \cdot g^{-1}$, respectively. The adsorption capacity of MIL-101(Cr)/AC for Cr(VI) was 47.00 $mg \cdot g^{-1}$, which was higher than that of AC (45.22 $mg \cdot g^{-1}$) but less than that of MIL-101(Cr) (50.5 $mg \cdot g^{-1}$). The adsorption of Cr(VI) on MIL-101(Cr)/AC is a spontaneous exothermic process and best fitted with the second-order kinetic model and Langmuir isotherm model. The composite of MIL-101(Cr)/AC, is a green adsorbent and shows good reusability for Cr(VI) removal from water.

Keywords: Adsorption; *In-situ* synthesis; Activated carbon; Cr(III); Cr(VI); MIL-101(Cr)

1. Introduction

Due to continuous industrialization, heavy metal pollution is becoming increasingly serious, and toxic heavy metals have become one of the main pollutants in wastewater treatment. Common heavy metal pollutants include lead, chromium, arsenic, mercury and nickel, among them chromium is extremely toxic, carcinogenic and non-biodegradable, which is mainly used in many industrial processes and widely exists in the living environment [1]. Treatment of chromium-containing wastewater faces many challenges. Trivalent chromium (Cr(III)) and hexavalent chromium (Cr(VI)) are two main forms of chromium, of which Cr(III) is less toxic than Cr(VI) and can cause harm to human body when accumulated in a large amount, while the toxicity of Cr(VI) is much greater than that of Cr(III) [2,3]. Since, it can enter the plant body and accumulate with water circulation, and then through the food chain threaten the human health and even can lead to death [4]. Thus, heavy metal removal in wastewater is particularly important.

At present, the treatment of Cr(VI) is focused mainly on absorption or reduction to Cr(III) via different method such as adsorption [5], ion-exchange [6], electrochemistry [7], biological treatment [8], photocatalysis [9] and other technologies to reduce its toxicity. Among them, adsorption is seen as one of the most effective and widely used methods to treat Cr(VI), which is highly favored by researchers [10]. Common adsorbents include zeolite [11], active carbon [12], biomass [13], graphene oxide [14], etc., among them active carbon has become one of the most widely used adsorbents due to its advantages of green adsorption, non-toxic, low cost and high efficiency [15]. However, most adsorbents have

* Corresponding author.

the problems of subsequent treatment and secondary pollution while effectively removing pollutants. Apart from that, although the behavior of Cr(VI) reduced to Cr(III) can lower toxicity, the resource cannot be fully utilized, and Cr(III), as a toxic substance, cannot be effectively treated. Therefore, for the subsequent problems of heavy metal treatment, resource utilization can be considered, which means that the adsorbent after adsorption of heavy metal ions is separated for reuses, so that a new composite material is synthesized and used for removing heavy metals in wastewater.

Metal–organic frameworks (MOFs) is a sort of porous crystalline materials with periodic structure, which can be composed through self-assembly of metal ions/metal centers and organic linkers/bridging ligands [16], and has become an attractive material in different fields including adsorption [17,18]. Compared with traditional porous materials like activated carbon, MOFs has high specific surface area, low density, large porosity, uniform dispersion structure, abundant active sites and modifiable functional groups, and its adjustable pore structure and surface properties provide a good foundation for further development and utilization of new adsorbents [19]. There are many types of MOF materials, among them the chromium-based metal organic framework material MIL-101(Cr) is a extremely stable mesoporous super tetrahedral unit composed of Cr(III) and terephthalate ligands [20]. Being one of the representative MOFs materials, MIL-101(Cr) has excellent performance in treating pollutants in wastewater due to its rich active sites, special skeleton structure and surface charges, which provides new value for wastewater treatment [21]. MIL-101(Cr) can be compounded with suitable substances to enhance the performance of the original material. Hasanzadeh et al. [22] prepared a nano porous composite AC@MIL-101(Cr) in a simple hydrothermal method, and compared with single MIL-101(Cr) and activated carbon (AC), the composite AC@MIL-101(Cr) with higher specific surface area and pore volume showed better adsorption capacity. After 90 min, the adsorption efficiency of DR31 and AB92 by AC@MIL-101(Cr) was 99.4% and 92.9%, respectively. Aldawsari et al. [23] developed a porous adsorbent material (AC-NH2-MIL-101(Cr)) for PNP removal. And the adsorption of AC-NH2-MIL-101 for PNP was greatly improved compared with that of monomer.

Therefore, in this paper, Cr(III) in simulated wastewater was adsorbed and separated by activated carbon (AC), and AC after full adsorption of Cr(III) was used as the chromium source to prepare the chromium-based metal organic framework material MIL-101(Cr)/AC composite for Cr(VI) removal in wastewater. The main objectives were as follows: (1) treatment of Cr(III) wastewater by AC and utalization of waste as green resouce; (2) to develop a novel green adsorbent composite MIL-101(Cr)/AC by adsorption separation *in-situ* syntehsis to regenerate and reuse AC; (3) to explore the adsorptive property and behavior of MIL-101(Cr)/AC for Cr(VI) removal, and provide a new idea for wastewater treatment.

2. Experimental setup

2.1. Reagents and instruments

Activated carbon, chromium nitrate nonahydrate ($Cr(NO_3)_3{\cdot}9H_2O$), N,N-dimethylformamide (DMF), terephthalic acid, diphenyl carbazide, hydrofluoric acid, potassium chromate as heavy metal, hydrochloric acid and sodium hydroxide were purchased from Shenning Taixi Carbon-Based Industry Co., Ltd., Sinopharm Chemical Reagent Co., Ltd., Fuchen (Tianjin) Chemical Reagent Co., Ltd., Tianjin Fuchen Chemical Reagent Factory, Tianjin Fuyu Fine Chemical Co., Ltd., Tianjin Hedong Hongyan Reagent Factory, China, Xi'an Chemical Reagent Factory, China, Xi'an Sanpu Fine Chemical Factory of China, respectively. All the chemical agents were analytical grade.

The structure and the composition of the adsorbent was identified by X-ray powder diffraction (XD-3, Universal Analysis, Beijing, Cu-Kα radiation, 40 kV, 40 mA, λ¼ 0.15418 nm). The chemical structure of materials was analyzed by Fourier-transform infrared spectroscopy (KBr, Perkin-Elmer 550S, PerkinElmer, United States). The surface morphology was detected by scanning electron microscope (JSM-6710F, JEOL, Japan). The specific surface area and pore structure of the material were investigated using N_2 physical adsorption analyzer (ASAP 2020, Micromeritics, USA).

2.2. Adsorption separation

For adsorption of Cr(III) by AC, a certain amount of $Cr(NO_3)_3{\cdot}9H_2O$ was dissolved in deionized water and AC was put into it, oscillated for 24 h at room temperature, then the adsorption saturated AC was obtained.

2.3. MIL-101(Cr)/AC synthesis in-situ

Appropriate amount of H_2BDC (0.042 g) and AC separated above were dissolved in aqueous solution, then a certain amount of hydrofluoric acid (0.01 mL, 40%) was added, stirred at room temperature to get homogenous mixture and then reacted at 220°C for 12 h in a Teflon lined autoclave (100 mL). After that washed three times with DMF and ethanol and further washed with deionized water for another three times. Then dried at 60°C, activated at 150°C for 12 h and MIL-101(Cr)/AC composite was obtained finally.

MIL-101(Cr) was prepared by hydrothermal method [24]. Briefly, 2.0 g $Cr(NO_3)_3{\cdot}9H_2O$ and 0.83 g terephthalic acid were mixed in 20 mL deionized water, while adding 0.2 mL 40% of hydrofluoric acid dropwise, stirred for 30 min to get a homogenous mixture of the solution. Then following the same steps of the above MIL-101(Cr)/AC to obtain the purified MIL-101(Cr) sample.

2.4. Adsorption experiments

2.4.1. Adsorption kinetics

For studying the adsorption kinetic, the solution of 20 mg AC, MIL-101(Cr) and MIL-101(Cr)/AC were mixed into 100 mL (30 mg·L^{-1}) Cr(VI) solution, respectively. The contaminate was filtered and separated at 25°C for different time and the concentration of Cr(VI) was tested.

2.4.2. Adsorption isotherm

The solution of 100 mL of Cr(VI) was prepared by adding 20 mg AC, MIL-101(Cr) and MIL-101(Cr)/AC with different concentrations. The solution was placed in shaker at 25°C

for certain time and the supernatant was separated/filtered and the concentration of Cr(VI) was determined.

2.4.3. Adsorption thermodynamics

20 mg of AC, MIL-101(Cr) and MIL-101(Cr)/AC were put into 100 mL (30 mg·L^{-1}) Cr(VI) solution, respectively, and shook at various temperature. After the separation/filtering the concentration of Cr(VI) was detected.

2.4.4. Effects of pH, adsorbent dosage and temperature on adsorption

100 mL (20 mg·L^{-1}) Cr(VI) was prepared by adding AC, MIL-101(Cr) and MIL-101(Cr)/AC, respectively, vibrated for 3 h at a certain temperature, filtered and separated, and detected the concentration of Cr(VI). The pH value of Cr(VI) solution was adjusted with 0.1 mol·L^{-1} HCl and NaOH.

The following formula was used to calculated the adsorption capacity:

$$q_e = \frac{(C_o - C_e)V}{m} \quad (1)$$

where q_e is the equilibrium adsorption capacity, mg·g^{-1}; C_0 is the initial concentration, mg·L^{-1}; C_e is the concentration at equilibrium, mg·L^{-1}; V is the volume in simulated solution, L; m is the mass of the materials, g.

2.5. Analysis method

Total chromium was determined by potassium permanganate oxidation diphenyl carbazide spectrophotometry, Cr(VI) was determined by diphenyl carbazide spectrophotometry and Cr(III) was determined by total chromium minus Cr(VI).

3. Results and discussion

3.1. Material characterization

3.1.1. X-ray diffraction analysis

Fig. 1 displays the X-ray diffraction spectrum of AC, MIL-101(Cr) and MIL-101(Cr)/AC. Observed from Fig. 1, MIL-101(Cr) has obvious diffraction peaks at 3.3°, 5.2°, 8.5° and 9.1° (2θ), which were in keeping with the position of characteristic peaks reported in pervious literatures [25,26], indicating that MIL-101(Cr) was successfully synthesized with complete crystal form. The main characteristic peaks of MIL-101(Cr) appeared in MIL-101(Cr)/AC material, although some characteristic peaks weaken slightly, the position of characteristic peaks did not change, which demonstrated that the composite of MIL-101(Cr)/AC material was successful.

3.1.2. Infrared spectrum analysis

Fig. 2 shows the infrared spectra of AC, MIL-101(Cr) and MIL-101(Cr)/AC. As displayed in the infrared spectrum of MIL-101(Cr), the peak at 1,627 cm^{-1} is related to the stretching vibration of C=O double bond in –COOH of terephthalic acid, the adsorption peaks at 1,539 and 1,394 cm^{-1} were the asymmetric stretching vibration and symmetric stretching vibration of carboxyl group, and the adsorption peak at 582 cm^{-1} was caused by the stretching vibration of Cr–O bond. Besides, the adsorption peaks at 600~1,600 cm^{-1} were related to the adsorption peaks of benzene ring, mainly including C=C at 1,508 cm^{-1}. The results illustrated that MIL-101(Cr) has been synthesized successfully [27,28]. In the infrared spectrum of MIL-101(Cr)/AC, the characteristic peak appeared in MIL-101(Cr), proven the existence of MIL-101(Cr) in MIL-101(Cr)/AC.

3.1.3. Scanning electron microscopy analysis

Fig. 3a–f presents the scanning electron microscopy images of AC, MIL-101(Cr) and MIL-101(Cr)/AC materials. Fig. 3a and b show that MIL-101(Cr) material is in good crystal formability with octahedral structure, uniform particles and smooth surface, which was in accorded with the structure of MIL-101(Cr) reported in reference [29]. From Fig. 3e and f it is found that MIL-101(Cr) on MIL-101(Cr)/AC changed the octahedral structure and was regularly stacked together to form a rod-shaped structure. The decrease of regularity and integrity of crystal indicated that *in-situ* synthesis on AC has an impact on the structure of MIL-101(Cr).

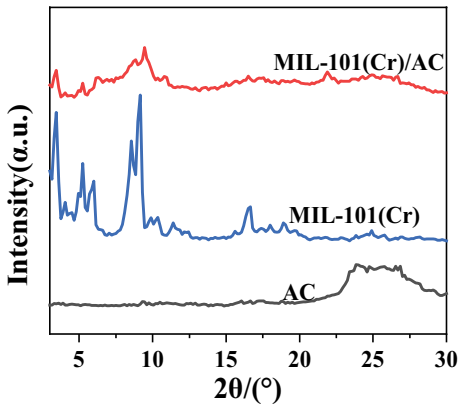

Fig. 1. X-ray diffraction spectrum of AC, MIL-101(Cr) and MIL-101(Cr)/AC.

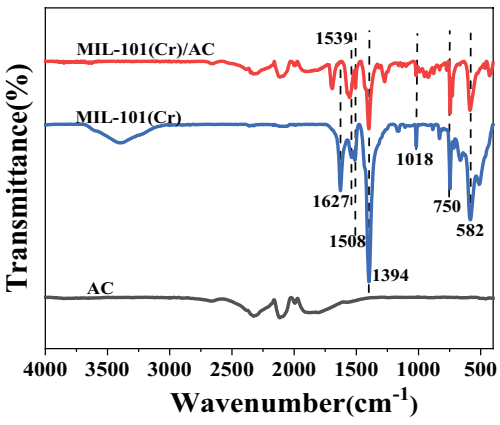

Fig. 2. Infrared spectrum of AC, MIL-101(Cr) and MIL-101(Cr)/AC.

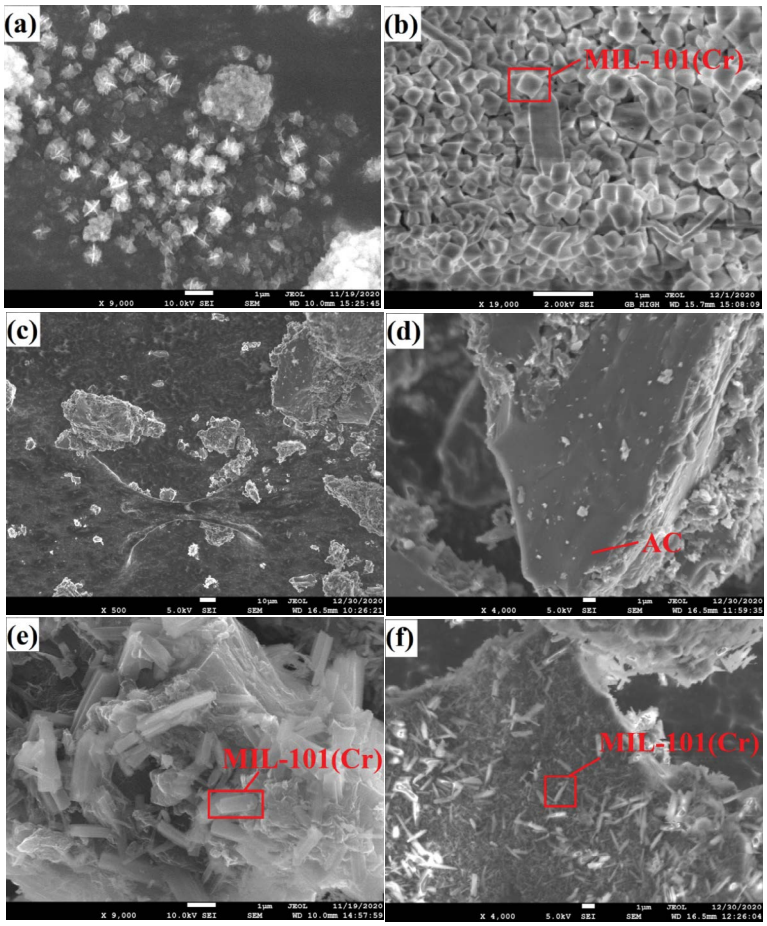

Fig. 3. Scanning electron microscopy images of MIL-101(Cr) (a,b), AC (c,d) and MIL-101(Cr)/AC (e,f).

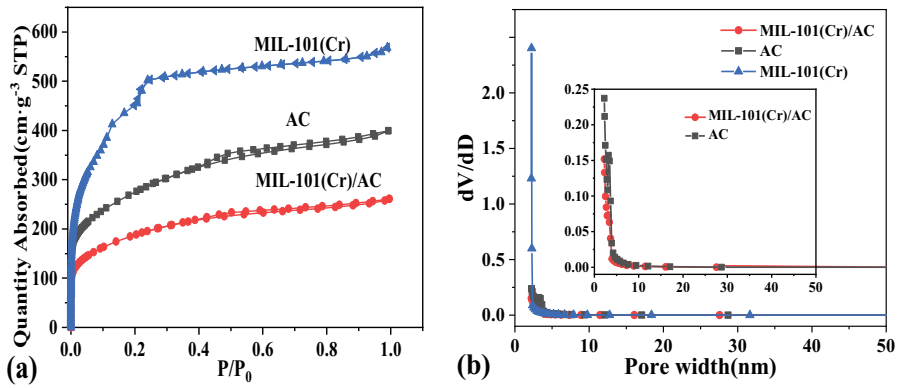

Fig. 4. N_2 adsorption–desorption isotherms (a) and pore-size distribution (b) of AC, MIL-101(Cr) and MIL-101(Cr)/AC.

3.1.4. Analysis of specific surface area and pore structure

Fig. 4 shows the N_2 adsorption–desorption isotherms (a) and pore-size distribution (b) of AC, MIL-101(Cr) and MIL-101(Cr)/AC, from which it can be concluded that AC showed very high N_2 saturation adsorption performance, and the N_2 saturation adsorption of MIL-101(Cr)/AC dropped sharply, indicating that the specific surface area of MIL-101(Cr)/AC was lower than that of AC. At the same time, the pore volume and pore size of MIL-101(Cr)/AC were obviously smaller. As the specific surface area parameters could be seen from Table 1, the data showed that the specific surface area, pore volume and pore size of MIL-101(Cr)/AC were reduced, which may be due to MIL-101(Cr) occupies the larger pore diameter of AC.

3.1.5. Analysis of zeta potential

Fig. 5 shows the zeta potential diagram of AC, MIL-101(Cr) and MIL-101(Cr)/AC. It's clearly shown that the

Table 1
Specific surface area and pore structure parameters of AC, MIL-101(Cr) and MIL-101(Cr)/AC

Adsorbent	Specific surface area ($m^2 \cdot g^{-1}$)	Pore volume ($cm^3 \cdot g^{-1}$)	Pore width (nm)
AC	950.9	0.62	2.60
MIL-101(Cr)	1,687.1	0.88	2.08
MIL-101(Cr)/AC	655.9	0.40	2.46

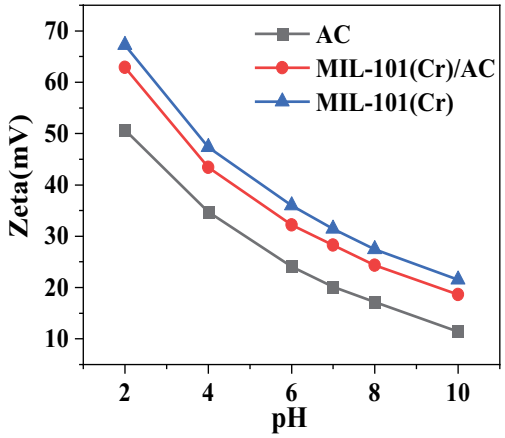

Fig. 5. Zeta potential diagram of AC, MIL-101(Cr) and MIL-101(Cr)/AC.

zata potential values of AC, MIL-101(Cr) and MIL-101(Cr)/AC were all positive when the solution pH was ranging from 2–10, indicating that the material surface was positively charged.

3.2 Adsorption of Cr(III) on AC

3.2.1. Effect of dosage on Cr(III) adsorption

Fig. 6 describes how the adsorbent dosage effect on the adsorption of Cr(III) on AC, from which can be seen that the adsorption ability of Cr(III) on AC was first rose and then decreased with the increase of the adsorbent dosage. When the concentration and volume of Cr(III) in solution were fixed, the less the adsorbent dosage was, the higher adsorption capacity would obtain. That was because the adsorbent per unit mass adsorbed more Cr(III), the adsorption capacity was higher. With adsorbent dosage increasing, the equilibrium adsorption capacity decreased, which was due to the fact that the material provides a much larger specific surface area and adsorption active sites under the condition of the same adsorbent concentration and volume, but the binding times of the adsorbent with Cr(III) per unit mass decreased, leading to the reduction of the adsorption capacity.

3.2.2. Effect of pH on Cr(III) adsorption

Fig. 7 presents the influence of pH on Cr(III) adsorption. Obviously, the adsorption effect of AC adsorbent on Cr(III) increased first, and then decreased with the increase

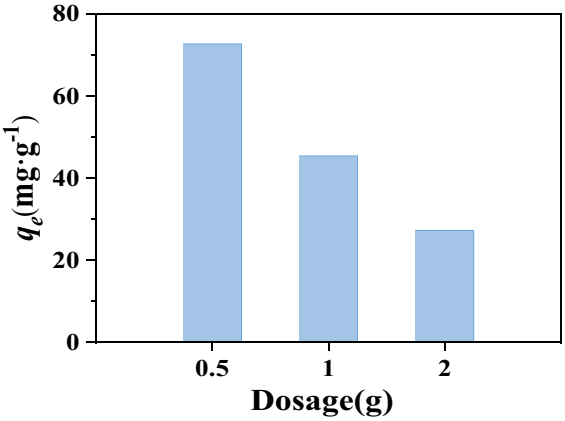

Fig. 6. Effect of dosage on adsorption of Cr(III) on AC.

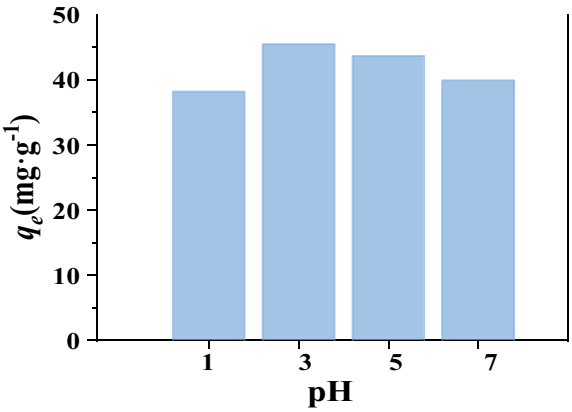

Fig. 7. Effect of pH on adsorption of Cr(III) on AC.

of pH value. When pH value was 3, the adsorption capacity of AC for the removal of Cr(III) reached to its high value. When the pH value was lower than 3, Cr(III) existed in the form of $(Cr(H_2O)_6)^{3+}$ in solution and had low binding capacity with the internal pores of AC, which was unfavorable to its diffusion in the AC pores and reduced the adsorption capacity. With pH value increasing, some Cr(III) and ionized hydroxyl ions formed complex ions $Cr(OH)^{2+}$ and $Cr(OH)_2^+$. Due to the smaller radius of complex ions and the lower positive charge, the mass transfer resistance was reduced to a certain extent, which was facilitated to the diffusion and chemical adsorption of Cr(III) in activated carbon pores. When the pH in the solution exceeded 3, Cr(III) begins to precipitate in the form of $Cr(OH)_3$.

3.2.3. Effect of coexisting (Ni^{2+} and Co^{2+}) on Cr(III) adsorption

Fig. 8 shows the effect of Ni^{2+} and Co^{2+} on Cr(III) adsorption by AC, indicating that the adsorption capacity of AC for Cr(III) removal was reduced due to the presence of co-existing ions. In the presence of Ni^{2+} ions, the adsorption capacity of AC for Cr(III) removal was decreased from 45.45 to 27.27 $mg \cdot g^{-1}$ with the increase of Ni^{2+}; in the presence of Co^{2+} ions, with the increase of Co^{2+}, the adsorption capacity of AC for Cr(III) removal was decreased from 45.45

to 9.09 mg·g^{-1}, indicating that the presence of coexisting ions had negative impact on Cr(III) adsorption. Meanwhile, compared with Ni^{2+}, the presence of Co^{2+} showed more negative effect on the adsorption process. The greater influence of Cr(III) was due to the smaller radius of the same valence ion, the greater the ion charge density, the greater the force on water molecules, the larger the solvent water molecular layer around the ion, and the larger the radius of hydrated ion, resulting in weak adsorption capacity [30,31]. The charge numbers of Ni^{2+} and Co^{2+} were the same, but the hydration radius of Co^{2+} was small. Thus, the influence of Co^{2+} on Cr(III) adsorption was greater than that of Ni^{2+}.

3.3. Adsorption experiment of Cr(VI) on MIL-101(Cr)/AC

3.3.1. Adsorption kinetics

Fig. 9 describes the effect of adsorption time on Cr(VI) removal. As displayed in Fig. 9, in the first 20 min during the process of adsorption, the adsorption capacity of AC, MIL-101(Cr) and MIL-101(Cr)/AC for Cr(VI) removal increased very fast, which was due to the high surface area, porous structure and large number of active sites of the materials [32]. As time progressed, most of the active sites were occupied gradually and the adsorption rate decreased slowly. 180 min later, the adsorption capacity was basically stable and reached the adsorption equilibrium. Compared with AC, the equilibrium adsorption capacity of MIL-101(Cr)/AC for Cr(VI) was increased about 4%, which was due to the effective of –OH and Cr(VI) in the inorganic chain of MIL-101(Cr)/AC adsorbent; as cation frameworks needs additional anions in the cavity or pore to balance the charge of main skeleton, while Cr(VI) is an oxygen-containing anion in solution, which completed the ion exchange of heavy metal oxygen-containing [33].

In order to further discuss the process of Cr(VI) adsorption on AC, MIL-101(Cr) and MIL-101(Cr)/AC adsorbents, the experimental parameters were fitted by Lagergren pseudo-first-order kinetic model and pseudo-second-order kinetic model, respectively.

The Lagergren first-order adsorption kinetic equation [34] is shown as follows:

$$\log\left(q_e - q_t\right) = \log q_e - \frac{k_1}{2.303}t \tag{2}$$

where: q_t represents the adsorption capacity at time t, mg·g^{-1}; k_1 is the first-order adsorption rate constant, min^{-1}; t is the adsorption time, min; q_e is the equilibrium adsorption capacity, mg·g^{-1}.

The second-order adsorption kinetic equation [35] is:

$$\frac{t}{q_t} = \frac{1}{k_2 q_e^2} + \frac{1}{q_e}t \tag{3}$$

where: k_2 is the second-order adsorption rate constant, g(mg·min)$^{-1}$.

The regression parameters are shown in Table 2 (where $q_{e,c}$ represents the calculated equilibrium adsorption capacity), from which can be seen that the adsorption progress of Cr(VI) on AC, MIL-101(Cr) and MIL-101(Cr)/AC was more coincident with the second-order kinetic model.

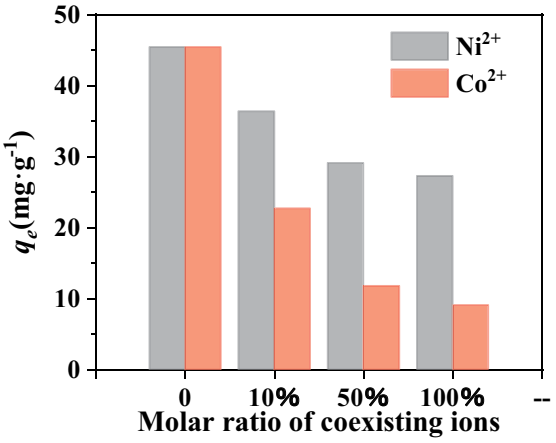

Fig. 8. Effect of Ni^{2+} and Co^{2+} on adsorption of Cr(III) on AC.

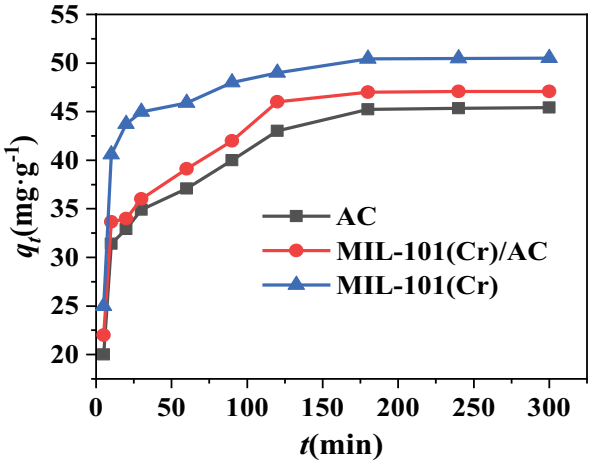

Fig. 9. Effect of adsorption time on Cr(VI) adsorption.

Table 2
Kinetic model parameters for the adsorption of Cr(VI) on AC, MIL-101(Cr) and MIL-101(Cr)/AC

Adsorbent	q_e (mg·g^{-1})	First-order kinetic model			Second-order kinetic model		
		k_1 (min^{-1})	$q_{e,c}$ (mg·g^{-1})	R^2	k_2 (g(mg·min)$^{-1}$)	$q_{e,c}$ (mg·g^{-1})	R^2
AC	45.22	0.0170	20.04	0.9287	0.0022	46.95	0.9988
MIL-101(Cr)	50.50	0.0281	19.22	0.9023	0.0038	51.28	0.9998
MIL-101(Cr)/AC	47.00	0.0219	22.66	0.9018	0.0023	48.54	0.9989

3.3.2. Adsorption isotherm

Fig. 10 describes the adsorption isotherms of Cr(VI) on samples. It is indicated that the adsorption ability of Cr(VI) increased with the increase of initial concentration and then gradually became stabilized. At lower initial concentration of Cr(VI), the adsorbent has enough adsorption sites, by increasing the initial concentration, the adsorption of Cr(VI) continuously filled the active sites of the material until basically saturated. The adsorption ability of Cr(VI) on AC is slightly lower than MIL-101(Cr)/AC when the concentration is the same.

The Langmuir and Freundlich isotherm adsorption models were devoted to process the data in Fig. 10. The relevant parameters are displayed in Table 3.

The Langmuir adsorption isotherm equation [36] is:

$$\frac{1}{q_e}=\frac{1}{Q^0}+\left(\frac{1}{bQ^0}\right)\left(\frac{1}{C_e}\right) \tag{4}$$

where Q^0 is the unit saturated adsorption capacity when monolayer adsorption is formed, mg·g^{-1}; C_e is the equilibrium mass concentration of the solution, mg·L^{-1}; q_e is the equilibrium adsorption capacity, mg·g^{-1}; b is the Langmuir equilibrium constant.

The Freundlich adsorption isotherm equation [37] is:

$$\log q_e=\log K_F+\frac{1}{n}\log C_e \tag{5}$$

where K_F and n are adsorption constants.

It can be found out from Table 3 that the adsorption behavior of Cr(VI) on AC, MIL-101(Cr) and MIL-101(Cr)/AC were more in line with the Langmuir adsorption isotherm, in which the linear correlation coefficients R^2 were greater than that of the Freundlich adsorption isotherm equation. Therefore, Cr(VI) adsorption on the adsorbent was monolayer adsorption.

3.3.3. Adsorption thermodynamics

Fig. 11 presents the influence of temperature on Cr(VI) adsorption, showing that as the temperature rose, the equilibrium adsorption capacity of Cr(VI) on AC, MIL-101(Cr) and MIL-101(Cr)/AC decreased.

The experimental data of Cr(VI) adsorption on AC, MIL-101(Cr) and MIL-101(Cr)/AC materials were analyzed and processed by the thermodynamic formula as follows [38]:

$$\Delta G=\Delta H-T\Delta S \tag{6}$$

where ΔG is the Gibbs free energy change, J·mol^{-1}; ΔH is the adsorption enthalpy change, J·mol^{-1}; ΔS is the adsorption entropy change, J(K·mol)$^{-1}$; T is thermodynamic temperature, K.

$$K_d=\frac{Q_e}{C_e} \tag{7}$$

where K_d is the distribution coefficient.

$$\log K_d=\frac{\Delta S}{R}-\frac{\Delta H}{2.303RT} \tag{8}$$

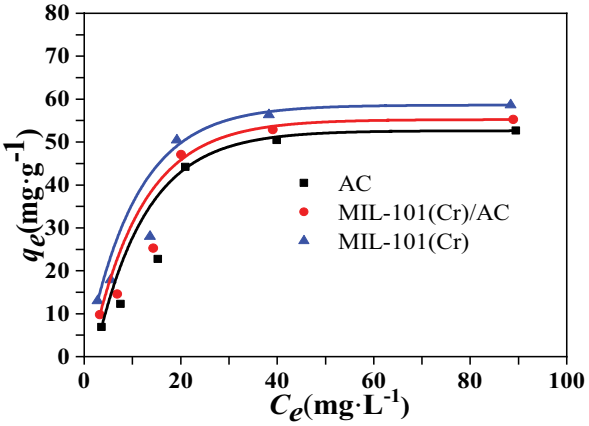

Fig. 10. Cr(VI) adsorption isotherms for samples.

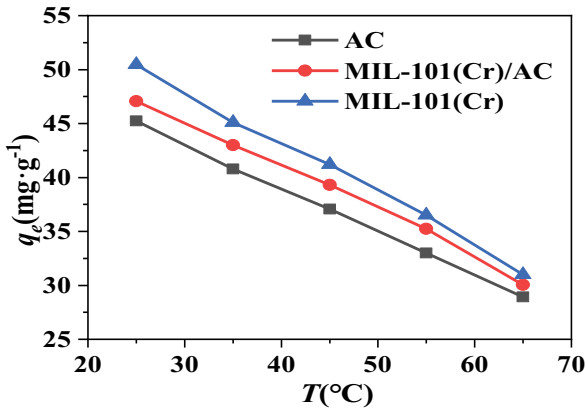

Fig. 11. Effect of temperature on Cr(VI) adsorption.

Table 3
AC, MIL-101(Cr) and MIL-101(Cr)/AC adsorption isotherm parameters of Cr(VI)

Adsorbent	Langmuir isotherm parameters			Freundlich isotherm parameters		
	Q^0 (mg·g^{-1})	b (L·mg^{-1})	R^2	K_F	n	R^2
AC	80.65	0.025	0.9582	3.04	1.41	0.8667
MIL-101(Cr)	59.17	0.094	0.9325	8.24	2.05	0.8990
MIL-101(Cr)/AC	112.36	0.023	0.9911	4.70	1.59	0.8815

where R is the thermodynamic constant, taking 8.314 J(K·mol)$^{-1}$.

The thermodynamic parameters that can be calculated according to Eqs. (5)~(7) are presented in Fig. 12 and Table 4. It can be calculated that the ΔH of the samples for the adsorption process of Cr(VI) was negative, indicating that the adsorption was an exothermic process; the value of ΔG was negative at different temperatures, meaning that it was a spontaneous process for Cr(VI) adsorption. The negative value of ΔS indicates that after Cr(VI) was adsorbed on the surface of MIL-101(Cr)/AC, the degree of freedom of the particle surface and the internal chaos of the reaction system were both reduced. In summary, the adsorption process of Cr(VI) by three materials is a spontaneous exothermic reaction.

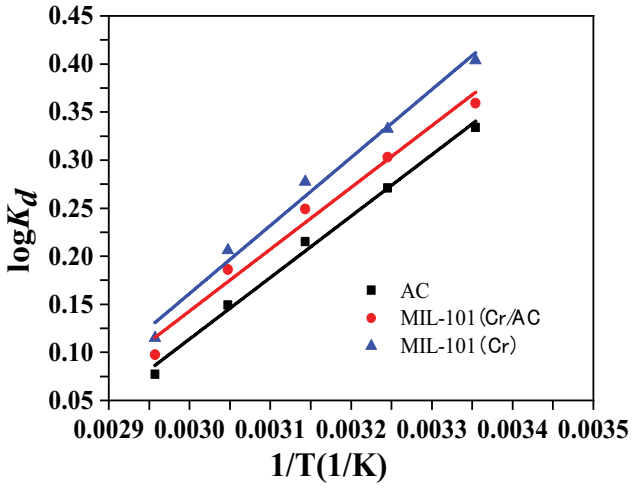

Fig. 12. LogK_d~1/T relation diagram of Cr(VI) adsorbed by samples.

Table 4
Thermodynamic parameters of Cr(VI) adsorption on samples

Adsorbent	T (K)	ΔG (kJ·mol^{-1})	ΔH (kJ·mol^{-1})	ΔS (J(K·mol)$^{-1}$)
	298.15	–7.51		
	308.15	–7.36		
AC	318.15	–7.21	–11.98	–15.00
	328.15	–7.06		
	338.15	–6.91		
	298.15	–8.68		
	308.15	–8.52		
MIL-101(Cr)	318.15	–8.36	–13.55	–16.31
	328.15	–8.19		
	338.15	–8.03		
	298.15	–7.88		
	308.15	–7.73		
MIL-101(Cr)/AC	318.15	–7.58	–12.31	–14.85
	328.15	–7.44		
	338.15	–7.29		

3.3.4. Effect of pH on Cr(VI) adsorption

The performance of Cr(VI) on AC, MIL-101(Cr) and MIL-101(Cr)/AC adsorbents under different pH conditions are described in Fig. 13. It can be seen that the adsorption capacity of Cr(VI) decreased with the increase of pH. At lower pH (acidic condition), Cr(VI) is mainly existed in the form of $HCrO^{4-}$, which interacts with anionic contaminants by electrostatic interaction when the adsorbent surface is positively charged; as the pH value increases, Cr(VI) exists with large quantities in the form of CrO_4^{2-} and the surface of the adsorbent was negatively charged, resulting in the electrostatic repulsion of anionic pollutants, which lowered the adsorption performance of Cr(VI) on the sorbent [39,40]. The adsorption ability of MIL-101(Cr)/AC on Cr(VI) was higher than that of AC, this is because at the same pH value, the positive charge of the surface of MIL-101(Cr)/AC was enhanced and at the same time the cation skeleton needs additional anions in the cavity or pore to balance the charged main skeleton, while Cr(VI) is an oxyanion in the solution, which just fulfils the ion exchange of the heavy metal oxyanion, thereby improving the Cr(VI) adsorption effect.

3.3.5. Effect of adsorbent dosage on Cr(VI) adsorption

The effect of dosage of the samples on Cr(VI) adsorption are shown in Fig. 14. As shown in Fig. 14, with the amount of the adsorbent increasing, the equilibrium adsorption capacity of Cr(VI) removal on samples gradually decreased. With the dosage increased, the specific surface area by the materials continued to increase, along with active adsorption sites being provided, but Cr(VI) content in the solution was finite, therefore the adsorption capacity per unit mass of adsorbent decrease when the amount of adsorbate remains unchanged.

3.3.6. Desorption regeneration

Fig. 15 shows the results of recycle adsorption experiments. After four times of adsorption–desorption process, the adsorption capacity of AC for Cr(VI) removal was decreased from 45.00 to 35.75 mg·g^{-1}; the adsorption

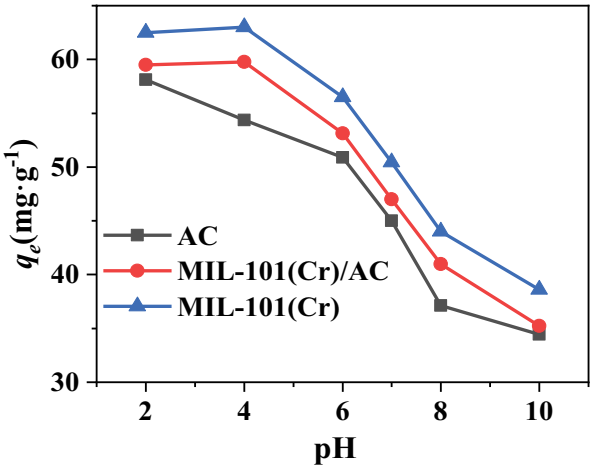

Fig. 13. Effect of pH on Cr(VI) adsorption.

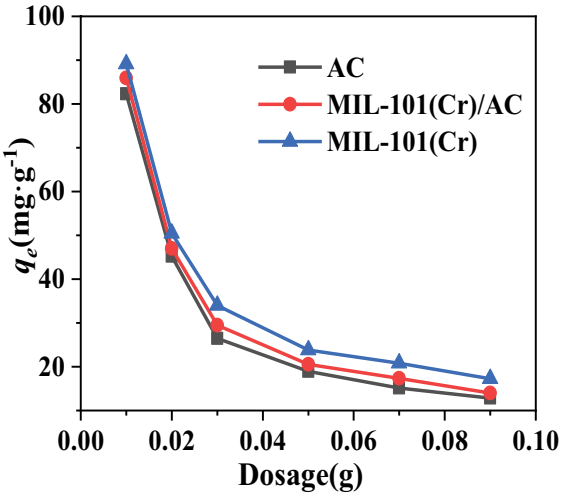

Fig. 14. Effect of the dosage on Cr(VI) adsorption.

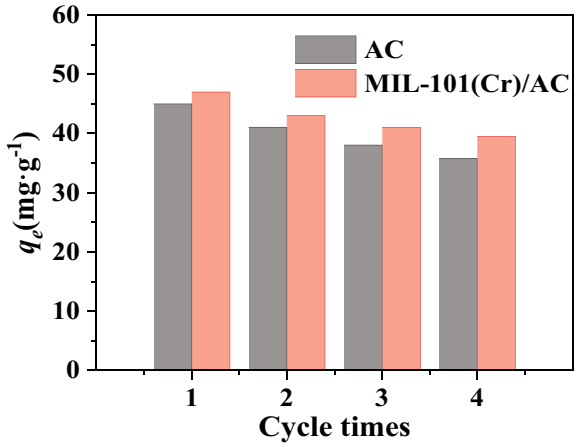

Fig. 15. Regeneration cycles of adsorbent materials.

capacity of MIL-101(Cr)/AC for Cr(VI) removal decreased from 47.00 to 39.49 mg·g^{-1}. It is obvious that the AC and MIL-101(Cr)/AC adsorbent still maintained their good adsorption performance for Cr(VI) removal after several cycles of regeneration.

4. Conclusion

In this work, a novel green MIL-101(Cr)/AC composite was synthesized *in-situ* successfully on the basis of the activated carbon (AC). The results indicated that the adsorption capacity of MIL-101(Cr)/AC for Cr(VI) removal was higher than that of AC. The adsorption kinetics experiment described that the adsorption process was monolayer adsorption. The adsorption isotherm experiment showed that the adsorption process was more in line with the Langmuir isotherm model. In addition, the adsorption thermodynamics experiment indicated that it is a behavior of self-exothermic for Cr(VI) adsorption on the samples. The fabricated composites displayed good reusability and maintain its efficient adsorption capacity after 4 cycles. In addition, the *in-situ* synthesized composite MIL-101(Cr)/AC enables waste pollutants to be reutilized.

CRediT authorship contribution statement

Zhuannian Liu: Conceptualization; Methodology, Project administration, Supervision, Funding acquisition. Yue Li: Methodology, Writing-original draft, Writing-review & editing. Yingying Teng: Methodology, Writing-original draft, Resources, Investigation.

Statements and declarations

Ethics approval

We assured that this manuscript is original work and this work neither accepted nor submitted simultaneously to any other journals.

Funding

This study was financially supported by the Key R&D projects of Shaanxi Province China (2022SF-578) and the Science and Technology Planning Project of Shaanxi Provincial Water Resources Department(2022slkj-5).

Competing interests

The authors declare that they have no known competing financial interests or personal relationships that could have appeared to influence the work reported in this paper.

References

[1] A. Fenti, S. Chianese, P. Iovino, D. Musmarra, S. Salvestrini, Cr(VI) sorption from aqueous solution: a review, Appl. Sci., 10 (2020) 6477, doi: 10.3390/app10186477.
[2] H. Karimi-Maleh, A. Ayati, S. Ghanbari, Y. Orooji, B. Tanhaei, F. Karimi, M. Alizadeh, J. Rouhi, L. Fu, M. Sillanpää, Recent advances in removal techniques of Cr(VI) toxic ion from aqueous solution: a comprehensive review, J. Mol. Liq., 329 (2021) 115062, doi: 10.1016/j.molliq.2020.115062.
[3] K.E. Ukhurebor, U.O. Aigbe, R.B. Onyancha, W. Nwankwo, O.A. Osibote, H.K. Paumo, O.M. Ama, C.O. Adetunji, I.U. Siloko, Effect of hexavalent chromium on the environment and removal techniques: a review, J. Environ. Manage., 280 (2021) 111809, doi: 10.1016/j.jenvman.2020.111809.
[4] M. Channegowda, Recent advances in environmentally benign hierarchical inorganic nano-adsorbents for the removal of poisonous metal ions in water: a review with mechanistic insight into toxicity and adsorption, Nanoscale Adv., 2 (2020) 5529–5554.
[5] P. Chen, Y. Wang, X. Zhuang, H. Liu, G. Liu, W. Lu, Selective removal of heavy metals by Zr-based MOFs in wastewater: new acid and amino functionalization strategy, J. Environ. Sci., 124 (2023) 268–280.
[6] Z. Ye, X. Yin, L. Chen, X. He, Z. Lin, C. Liu, S. Ning, X. Wang, Y. Wei, An integrated process for removal and recovery of Cr(VI) from electroplating wastewater by ion exchange and reduction–precipitation based on a silica-supported pyridine resin, J. Cleaner Prod., 236 (2019) 117631, doi: 10.1016/j.jclepro.2019.117631.
[7] V. Gopalakannan, S. Periyasamy, N. Viswanathan, Fabrication of magnetic particles reinforced nanohydroxyapatite/gelatin composite for selective Cr(VI) removal from water, Environ. Sci.-Water Res., 4 (2018) 783–794.

[8] A.M. Hamdan, H. Abd-El-Mageed, N. Ghanem, Biological treatment of hazardous heavy metals by *Streptomyces rochei* ANH for sustainable water management in agriculture, Sci. Rep., 11 (2021) 9314, doi: 10.1038/s41598-021-88843-y.
[9] C. Liu, P. Wang, Y. Qiao, G. Zhou, Self-assembled Bi_2SeO_5/rGO/MIL-88A Z-scheme heterojunction boosting carrier separation for simultaneous removal of Cr(VI) and chloramphenicol, Chem. Eng. J., 431 (2022) 133289, doi: 10.1016/j.cej.2021.133289.
[10] C. Han, L. Yang, H. Yu, Y. Luo, X. Shan, The adsorption behavior and mechanism of Cr(VI) on facile synthesized mesoporous NH-SiO_2, Environ. Sci. Pollut. Res., 27 (2020) 2455–2463.
[11] S. Dasgupta, M. Das, M.A. Klunk, S.J. Siqueira Xavier, N.R. Caetano, P.R. Wander, Copper and chromium removal from synthetic textile wastewater using clay minerals and zeolite through the effect of pH, J. Iran Chem. Soc., 18 (2021) 3377–3386.
[12] F. Ghorbani, S. Kamari, S. Zamani, S. Akbari, M. Salehi, Optimization and modeling of aqueous Cr(VI) adsorption onto activated carbon prepared from sugar beet bagasse agricultural waste by application of response surface methodology, Surf. Interfaces, 18 (2020) 100444, doi: 10.1016/j.surfin.2020.100444.
[13] H. Wang, N. Yang, M. Qiu, Adsorption of Cr(VI) from aqueous solution by biochar-clay derived from clay and peanut shell, Int. J. Inorg. Mater., 35 (2020) 301–308.
[14] A.M. Omer, E.M.A. El-Monaem, A.S. Eltaweil, Novel reusable amine-functionalized cellulose acetate beads impregnated aminated graphene oxide for adsorptive removal of hexavalent chromium ions, Int. J. Biol. Macromol., 208 (2022) 925–934.
[15] R. Reshmy, E. Philip, A. Madhavan, A. Pugazhendhi, R. Sindhu, R. Sirohi, M.K. Awasthi, A. Pandey, P. Binod, Nanocellulose as green material for remediation of hazardous heavy metal contaminants, J. Hazard. Mater., 424 (2022) 127516, doi: 10.1016/j.jhazmat.2021.127516.
[16] M. Lv, W. Zhou, H. Tavakoli, C. Bautista, J. Xia, Z. Wang, X. Li, Aptamer-functionalized metal-organic frameworks (MOFs) for biosensing, Biosens. Bioelectron., 176 (2021) 112947, doi: 10.1016/j.bios.2020.112947.
[17] Y.-Z. Li, G.-D. Wang, L.-N. Ma, L. Hou, Y.-Y. Wang, Z. Zhu, Multiple functions of gas separation and vapor adsorption in a new MOF with open tubular channels, ACS Appl. Mater. Interfaces, 13 (2021) 4102–4109.
[18] Y. Sakamaki, M. Tsuji, Z. Heidrick, O. Watson, J. Durchman, C. Salmon, S.R. Burgin, M.H. Beyzavi, Preparation and applications of metal-organic frameworks (MOFs): a laboratory activity and demonstration for high school and/or undergraduate students, J. Chem. Educ., 97 (2020) 1109–1116.
[19] W. Dong, H. Zhou, B. Mao, Z. Zhang, Y. Liu, Y. Liu, F. Li, D. Zhang, D. Zhang, W. Shi, Efficient MOF-derived V-Ni_3S_2 nanosheet arrays for electrocatalytic overall water splitting in alkali, Int. J. Hydrogen Energy, 46 (2021) 10773–10782.
[20] S.C. Tan, F.I.B. Zulkifli, H.K. Lee, Solvent-loaded metal-organic framework of type MIL-101(Cr)-NH_2 for the dispersive solid-phase extraction and UHPLC-MS/MS analysis of herbicides from paddy field waters, Microchim. Acta, 188 (2021) 046615, doi: 10.1007/s00604-020-04661-5.
[21] M. Zou, M. Dong, T. Zhao, Advances in metal-organic frameworks MIL-101(Cr), Int. J. Mol. Sci., 23 (2022) 169396, doi: 10.3390/ijms23169396.
[22] M. Hasanzadeh, A. Simchi, H.S. Far, Nanoporous composites of activated carbon-metal organic frameworks for organic dye adsorption: synthesis, adsorption mechanism and kinetics studies, J. Ind. Eng. Chem., 81 (2020) 405–414.
[23] A.M. Aldawsari, I.H. Alsohaimi, H.M.A. Hassan, M.R. Berber, Z.E.A. Abdalla, I. Hassan, E.A.M. Saleh, B.H. Hameed, Activated carbon/MOFs composite: AC/NH_2-MIL-101(Cr), synthesis and application in high performance adsorption of p-nitrophenol, J. Saudi Chem. Soc., 24 (2020) 693–703.
[24] S. Kayal, A. Chakraborty, Activated carbon (type Maxsorb-III) and MIL-101(Cr) metal organic framework based composite adsorbent for higher CH_4 storage and CO_2 capture, Chem. Eng. J., 334 (2018) 780–788.
[25] H. Zhao, Q. Li, Z. Wang, T. Wu, M. Zhang, Synthesis of MIL-101(Cr) and its water adsorption performance, Microporous Mesoporous Mater., 297 (2020) 110044, doi: 10.1016/j.micromeso.2020.110044.
[26] W. Xu, L. Ye, W. Li, Z. Zhang, Modulation of MIL-101(Cr) morphology and selective removal of dye from water, J. Iran Chem. Soc., 18 (2021) 159–166.
[27] K.A. Adegoke, O.S. Agboola, J. Ogunmodede, A.O. Araoye, O.S. Bello, Metal-organic frameworks as adsorbents for sequestering organic pollutants from wastewater, Mater. Chem. Phys., 253 (2020) 123246, doi: 10.1016/j.matchemphys.2020.123246.
[28] M. Jouyandeh, F. Tikhani, M. Shabanian, F. Movahedi, S. Moghari, V. Akbari, X. Gabrion, P. Laheurte, H. Vahabi, M.R. Saeb, Synthesis, characterization, and high potential of 3D metal–organic framework (MOF) nanoparticles for curing with epoxy, J. Alloys Compd., 829 (2020) 154547, doi: 10.1016/j.jallcom.2020.154547.
[29] V. Kavun, M.A. van der Veen, E. Repo, Selective recovery and separation of rare earth elements by organophosphorus modified MIL-101(Cr), Microporous Mesoporous Mater., 312 (2021) 110747, doi: 10.1016/j.micromeso.2020.110747.
[30] L. Dong, J. Liang, Y. Li, S. Hunang, Y. Wei, X. Bai, Z. Jin, M. Zhang, J. Qu, Effect of coexisting ions on Cr(VI) adsorption onto surfactant modified *Auricularia auricula* spent substrate in aqueous solution, Ecotoxicol. Environ. Saf., 166 (2018) 390–400.
[31] S.M. Kamyab, S. Modabberi, C.D. Williams, A. Badiei, Synthesis of sodalite from sepiolite by alkali fusion method and its application to remove Fe^{3+}, Cr^{3+}, and Cd^{2+} from aqueous solutions, Environ. Eng. Sci., 37 (2020) 689–701.
[32] R. Baby, M.Z. Hussein, Ecofriendly approach for treatment of heavy-metal-contaminated water using activated carbon of kernel shell of oil palm, Materials, 13 (2020) 112627, doi: 10.3390/ma13112627.
[33] X. Zhao, X. Yu, X. Wang, S. Lai, Y. Sun, D. Yang, Recent advances in metal-organic frameworks for the removal of heavy metal oxoanions from water, Chem. Eng. J., 407 (2021) 127221, doi: 10.1016/j.cej.2020.127221.
[34] M. Zou, W. Dai, P. Mao, B. Li, J. Mao, S. Zhang, L. Yang, S. Luo, X. Luo, J. Zou, Integration of multifunctionalities on ionic liquid-anchored MIL-101(Cr): a robust and efficient heterogeneous catalyst for conversion of CO_2 into cyclic carbonates, Microporous Mesoporous Mater., 312 (2021) 110750, doi: 10.1016/j.micromeso.2020.110750.
[35] J. Wang, Y. Chen, T. Sun, A. Saleem, C. Wang, Enhanced removal of Cr(III)-EDTA chelates from high-salinity water by ternary complex formation on DETA functionalized magnetic carbon-based adsorbents, Ecotoxicol. Environ. Saf., 209 (2021) 111858, doi: 10.1016/j.ecoenv.2020.111858.
[36] S. Hussain, M. Kamran, S.A. Khan, K. Shaheen, Z. Shah, H. Suo, Q. Khan, A.B. Shah, W.U. Rehman, Y.O. Al-Ghamdi, U. Ghani, Adsorption, kinetics and thermodynamics studies of methyl orange dye sequestration through chitosan composites films, Int. J. Biol. Macromol., 168 (2021) 383–394.
[37] N. Popa, M. Visa, New hydrothermal charcoal TiO_2 composite for sustainable treatment of wastewater with dyes and cadmium cations load, Mater. Chem. Phys., 258 (2021) 123927, doi: 10.1016/j.matchemphys.2020.123927.
[38] A. Saravanan, P.S. Kumar, S. Varjani, S. Karishma, S. Jeevanantham, P.R. Yaashikaa, Effective removal of Cr(VI) ions from synthetic solution using mixed biomasses: kinetic, equilibrium and thermodynamic study, J. Water Process Eng., 40 (2021) 101905, doi: 10.1016/j.jwpe.2020.101905.
[39] F.J. Goncalves, L.V. Alves Gurgel, L.C. Soares, F.S. Teodoro, G.M. Dias Ferreira, Y.L. Coelho, L.H. Mendes da Silva, D. Prim, L.F. Gil, Application of pyridine-modified chitosan derivative for simultaneous adsorption of Cu(II) and oxyanions of Cr(VI) from aqueous solution, J. Environ. Manage., 282 (2021) 111939, doi: 10.1016/j.jenvman.2021.111939.
[40] Y. Song, L. Wang, B. Lv, G. Chang, W. Jiao, Y. Liu, Removal of trace Cr(VI) from aqueous solution by porous activated carbon balls supported by nanoscale zero-valent iron composites, Environ. Sci. Pollut. Res., 27 (2020) 7015–7024.